Supporting Information

Portable visual assay of anthrax biomarker based on lanthanide coordination polymer nanoparticles and smartphone-integrated mini-device

Shengnan Yin [a]*, Tianlun Xu [b]

a, Institute for Advanced Study, Shenzhen University, Shenzhen 518060

b, College of Environmental and Resource Sciences, Zhejiang University, Hangzhou, 310058, China

*Corresponding Author. E-mail: snyin0204@163.com

Table of contents

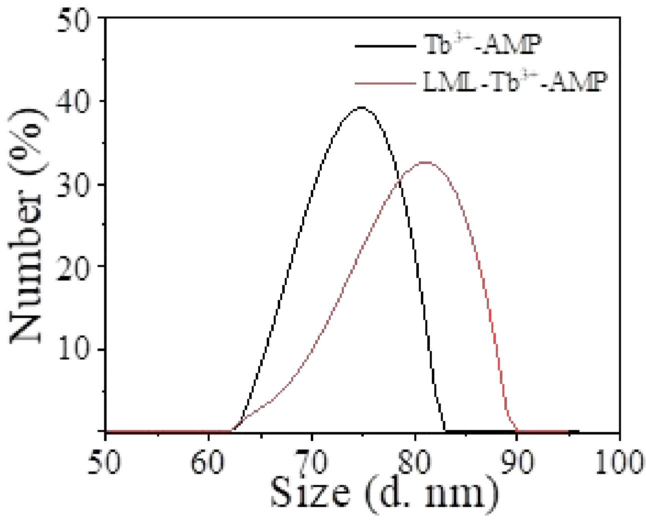

Figure S1 Particle size measured by DLS

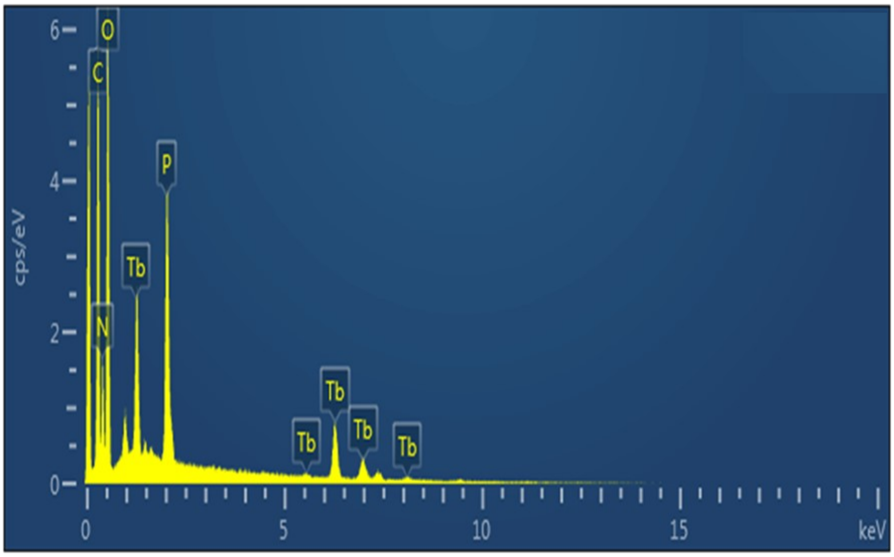

Figure S2 EDS spectra of LML-Tb^{3+}-AMP NPs

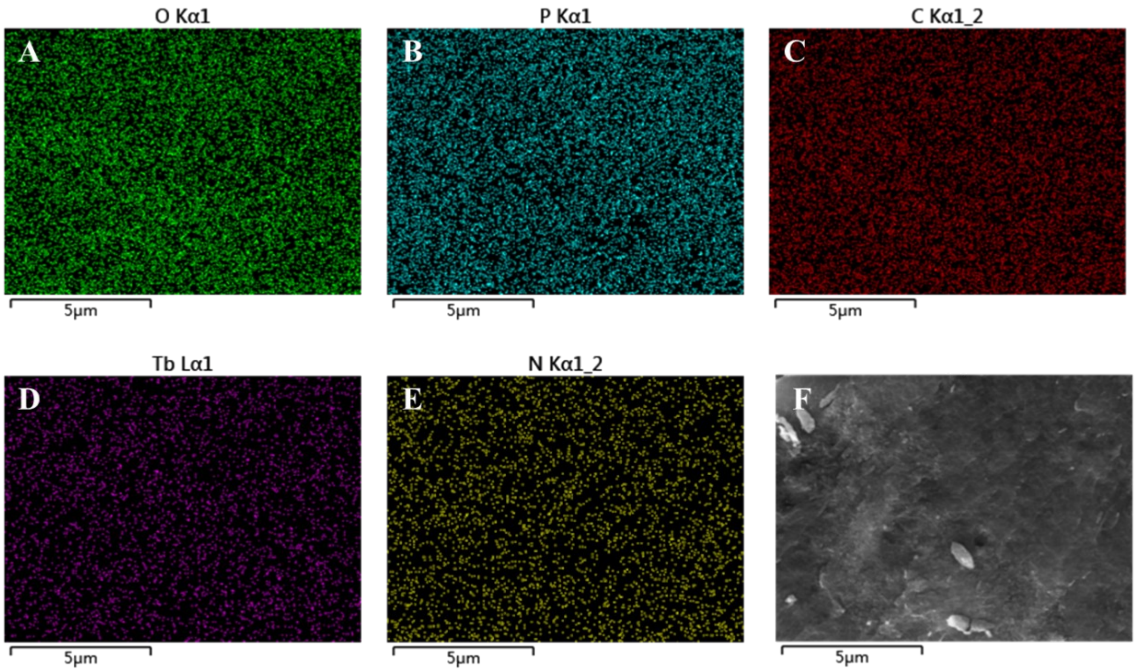

Figure S3 EDS mapping results of LML-Tb^{3+}-AMP NPs. (A) O, (B) P, (C) C, (D) Tb, (E) N, (F) SEM image of LML-Tb^{3+}-AMP NPs.

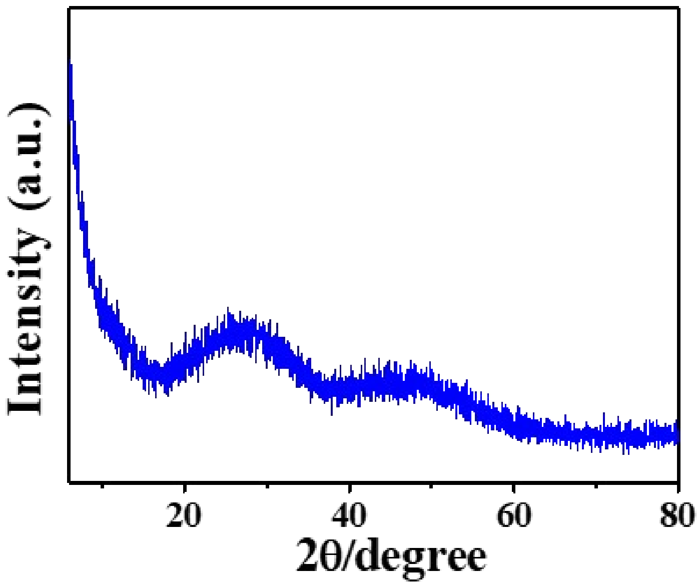

Figure S4 XRD pattern of LML-Tb^{3+}-AMP NPs.

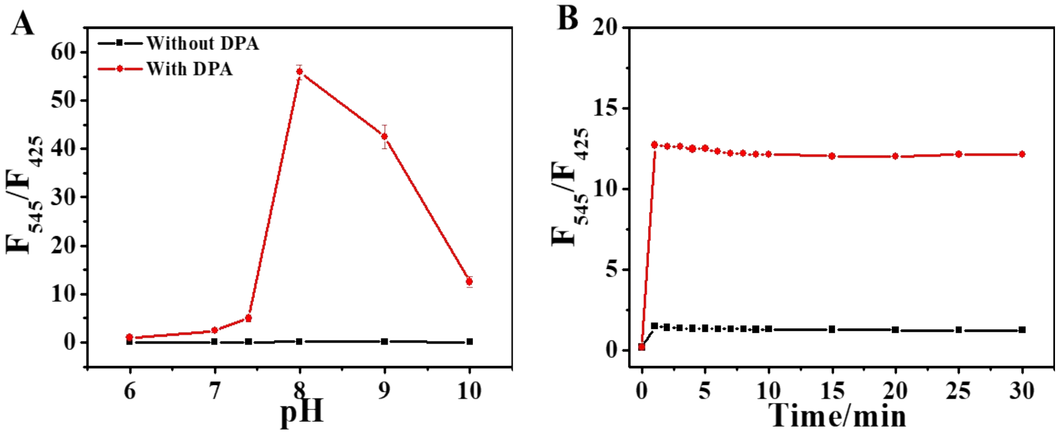

Figure S5 (A) Effect of pH on the fluorescence ratio (F_{545}/F_{425}) of LML-Tb^{3+}-AMP in the absence and presence of DPA. (B) Effect of equilibrium time on the fluorescence ratio (F_{545}/F_{425}) in the LML-Tb^{3+}-AMP system.

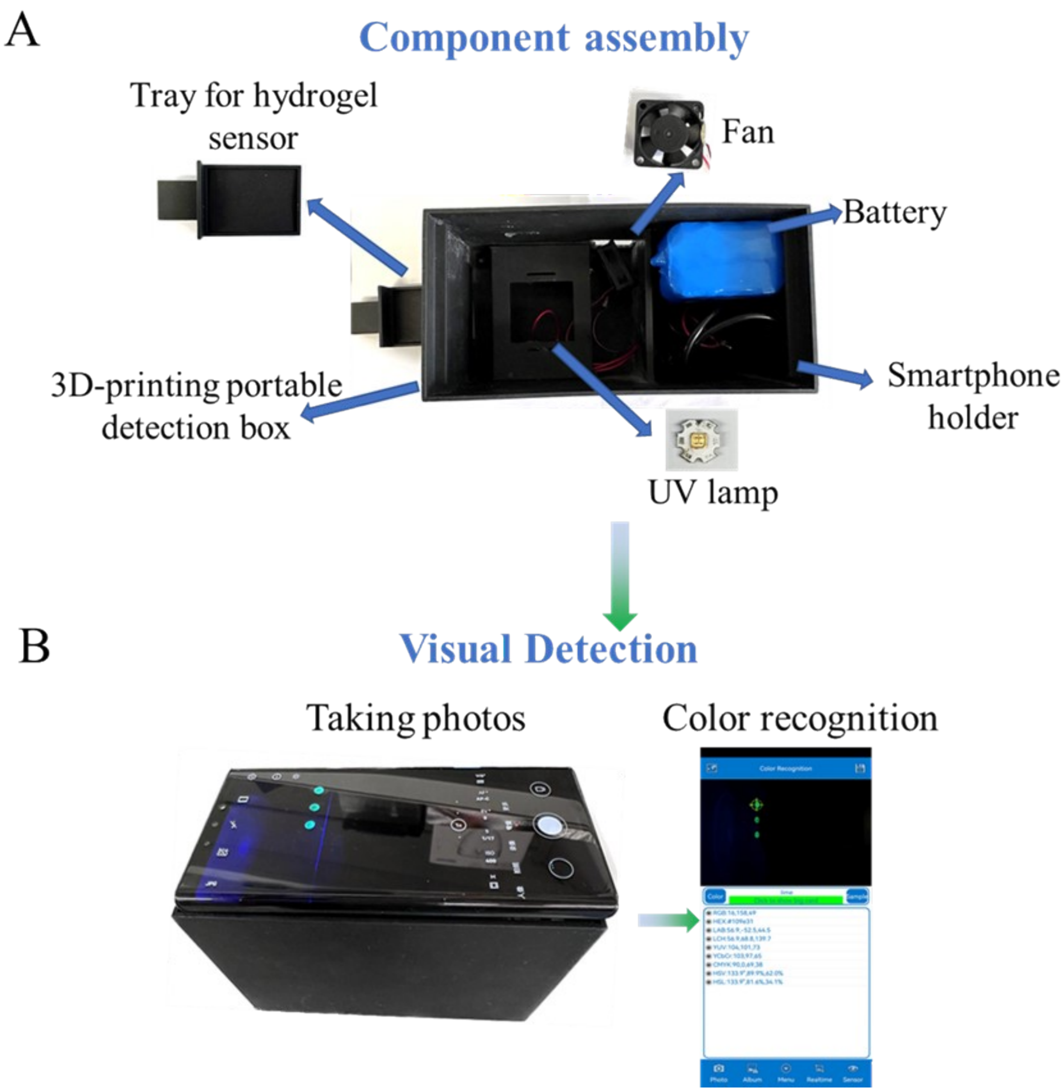

Figure S6 Schematic illustration of the (A) fabrication and composition, and (B) use of the portable detection device.

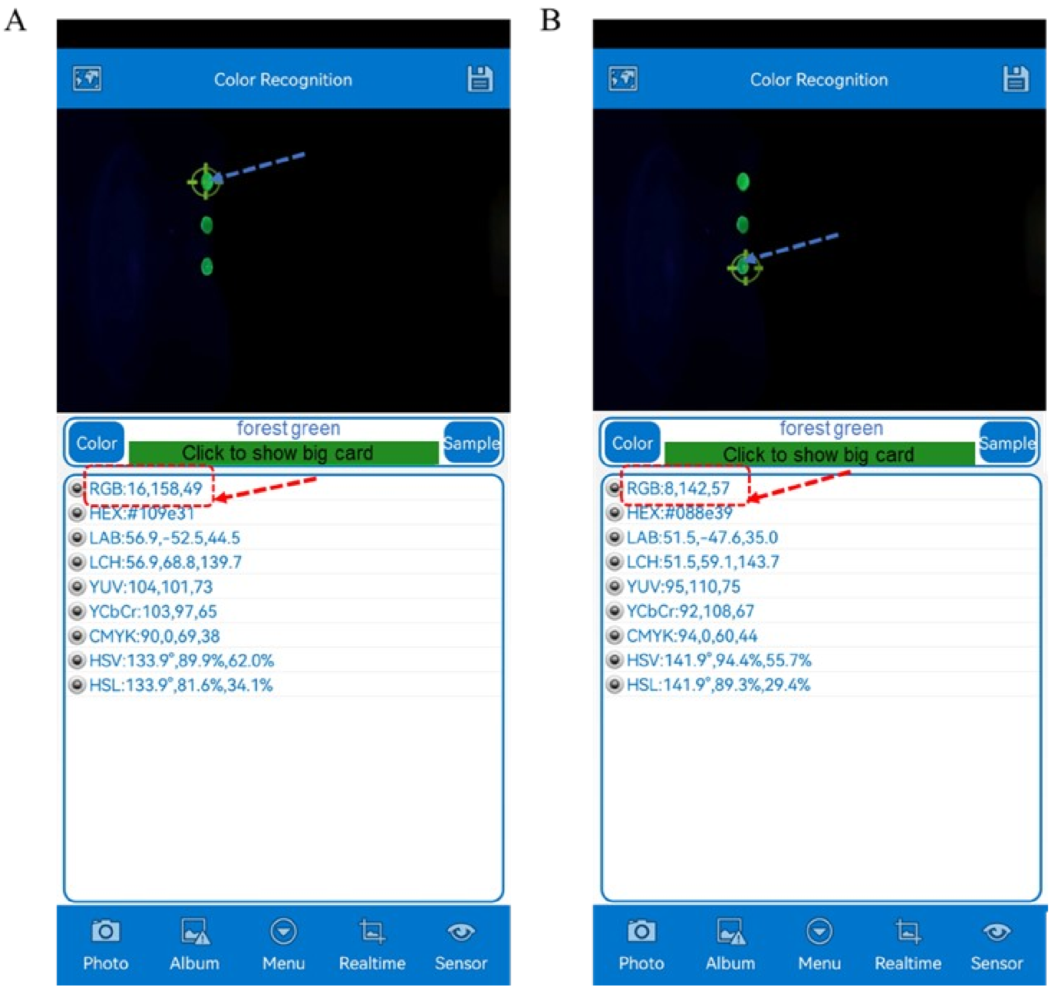

Figure S7 The RGB values recognized by smartphone APP (A and B) (the photograph was taken under 254 nm UV lamp).

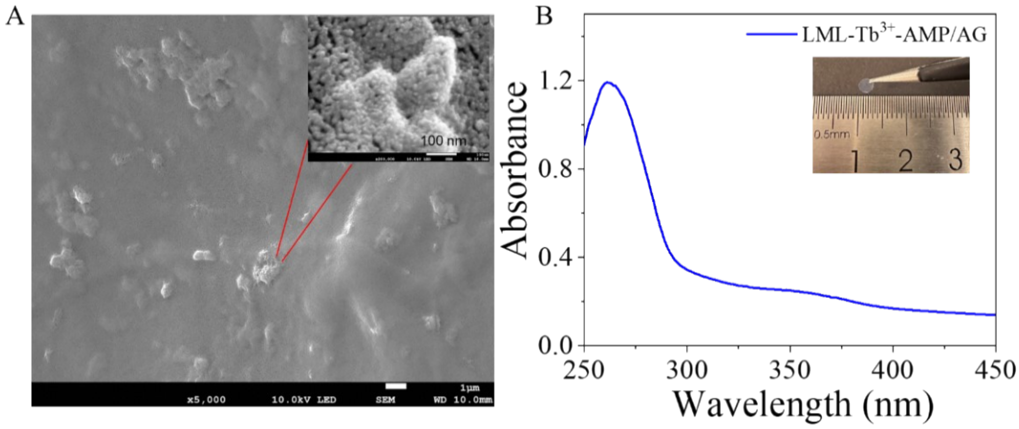

Figure S8. (A) SEM image of LML-Tb^{3+}- AMP/AG film. (B) UV-vis spectra of LML-Tb^{3+}- AMP/AG film. Inset: Image of the hydrogel sensor.

Table S1 The singlet and triplet energy levels of DPA and the lowest emission level of Tb^{3+}.

Sensitizer	S_1(cm^{-1})	T_1(cm^{-1})	ΔE_{ST} (cm^{-1})	$\Delta E_{TD\text{-}Tb}$ (cm^{-1})	Tb^{3+} ($^5D_4$, cm^{-1})
DPA	32722.6	26364.5	6358.1	5864.0	20500.5

The lowest emission levels of Ln^{3+} were obtained from ref. [1]

S_1: Lowest excited singlet; **T_1:** Lowest excited triplet; $\Delta \boldsymbol{E_{ST}}$**:** The energy gap between S_1 and T_1; $\Delta \boldsymbol{E_{TD\text{-}Tb}}$**:** the energy differences between the lowest triplet excited state of sensitizer and the emission levels of Tb^{3+}.

Table S2 Comparison in the sensitivity performance for DPA detection between the proposed method and the previously reported methods.

Sensing system	Mode	Linear range (μM)	LOD (nM)	Ref.
Tb^{3+}-GMP-Eu^{3+}	Ratiometric	2-16	96	[1]
His@ZIF-8/Tb^{3+}	Turn-on	0-10	20	[2]
EBT @ CDs/Eu^{3+}	Ratiometric	0.5-110	10.6	[3]
Tb^{3+} @ UIO-67	Ratiometric	0.3–6	36	[4]
Fe_3O_4 @ Tb^{3+}	Turn-on	0–1	5.4	[5]
R6G/Eu-CdS@ZIF-8	Ratiometric	0.1-150	67	[6]
Tb/Eu -BTC	Ratiometric	0.05-3	4.9	[7]
g-C_3N_4-Eu^{3+}-Cit	Ratiometric	0.1-15	13	[8]
LML-Tb^{3+}-AMP	Ratiometric	0.01–10	3.4	This work

Table S3 Determination of DPA in real samples

Samples	Added	Found (μM)	Recovery (%)	RSD (%)
Lake water 1	0.00	ND[a]	—	—
	0.50	0.51	110.0	2.8
	5.00	5.12	103.7	0.4
Lake water 2	0.00	ND[a]	—	—
	0.50	0.49	97.9	1.6
	5.00	5.01	100.2	0.8

[a] Not detected.

Table S4 Comparison in the sensitivity performance for DPA detection between the proposed method and the previously reported smartphone-based sensing method.

Sensing system	Mode	Linear range	LOD	Ref.
EBT @ CDs/Eu^{3+}	Ratiometric	0-12μM	0.68μM	[3]
g-C_3N_4-Eu^{3+}-Cit	Ratiometric	0-20μM	2.5μM	[8]
Tb-PTA-OH	Ratiometric	0-40 μM	0.48μM	[9]
Tb-GSH-CuNCs	Turn-on	0.5-70μM	0.5μM	[10]
Tb^{3+}@JUC-505	Turn-on	0-100μM	2.17μM	[11]
HAp:Tb-EDTA	Ratiometric	0.1-500 μM	0.5μM	[12]
UiO-66-NH_2/Eu	Ratiometric	0-35μM	0.52μM	[13]
Eu-MOF@Tb	Ratiometric	—	2μM	[14]
LML-Tb^{3+}-AMP	Ratiometric	0–100 μM	0.24μM	This work

References

[1] N. Gao, Y. F. Zhang, P. C. Huang, Z. H. Xiang, F. Y. Wu and L. Q. Mao, Perturbing tandem energy transfer in luminescent heterobinuclear lanthanide coordination polymer nanoparticles enables real-time monitoring of release of the anthrax biomarker from bacterial pores, *Anal. Chem.*, 2018, **90**, 7004−7011.

[2] L. Guo, M. Liang, X. Wang, R. Kong, G. Chen, L. Xia, and F, Qu, The role of l-histidine as molecular tongs: a strategy of grasping Tb^{3+} using ZIF-8 to design sensors for monitoring an anthrax biomarker on-the-spot, *Chem. Sci.*, 2020, **11**, 2407-2413.

[3] Q. Zhou, Y. Fang, J. Li, D. Hong, P. Zhu, S. Chen and K. Tan, A design strategy of dual-ratiomentric optical probe based on europium-doped carbon dots for colorimetric and fluorescent visual detection of anthrax biomarker, *Talanta*, 2021, **222**, 121548.

[4] X. Zhang, W. Zhang, G. Li, Q. Liu, Y. Xu and X. Liu, A ratiometric fluorescent probe for determination of the anthrax biomarker 2,6-pyridinedicarboxylic acid based on a terbium(III)−functionalized UIO-67 metal-organic framework, *Microchim. Acta*, 2020, **187**, 122.

[5] T. M. Koo, M. J. Ko, B. C. Park, M. S. Kim and Y. K. Kim, Fluorescent detection of dipicolinic acid as a biomarker in bacterial spores employing terbium ion-coordinated magnetite nanoparticles, *J. Hazard. Mater.,* 2021, **408**, 124870.

[6] X. Q. Li, J. J. Luo, L. Deng, F. H. Ma and M. H. Yang, In situ incorporation of fluorophores in zeolitic imidazolate framework-8 (ZIF-8) for ratio-dependent detecting a biomarker of anthrax spores, *Anal. Chem.*, 2020, **92**, 7114−7122.

[7] M. Wu, Z. W Jiang, P. Zhang, X. Gong and Y. Wang, Energy transfer-based ratiometric fluorescence sensing anthrax biomarkers in bimetallic lanthanide metal-organic frameworks, *Sensor Actuat. B-Chem*., 2023, **383**, 133596.

[8] M. Yuan, Y. Jin, L. Yu, Y. M. Bu, M. T. Sun, C. Yuan and S. H. Wang. Europium-modified carbon nitride nanosheets for smartphone-based fluorescence sensitive recognition of anthrax biomarker dipicolinic acid, *Food Chem*., 2023, **398**, 133884.

[9] L. Yu, L. X. Feng, L. Xiong, S. Li, S. Wang, Z. Y. Wei and Y. X. Xiao, Portable visual assay of Bacillus anthracis biomarker based on ligand-functionalized dual-emission lanthanide metal-organic frameworks and smartphone-integrated mini-device, *J. Hazard. Mater*, 2022, **434**, 128914.

[10] S. Pu, C. Shi, C. Lv, K. Xu, X. Hou and L. Wu, Tb^{3+}-based off–on fluorescent platform for multicolor and dosage-sensitive visualization of bacterial spore marker, *Anal.Chem.*, 2023, **95**, 8137-8144.

[11] Y. Liu, M. Wang, Y. Hui, L. Sun, Y. Hao, H. Ren, H. Guo and W. Yang, Polyarylether-based COFs coordinated by Tb^{3+} for the fluorescent detection of anthrax-biomarker dipicolinic acid, *J. mater. Chem. B*, 2023, DOI: 10.1039/d3tb02070c.

[12] C. Lv, S. Pu, L. Wu and X. Hou, Self-calibrated HAp:Tb-EDTA paper-based probe with dual emission ratio fluorescence for binary visual and fluorescent detection of anthrax biomarker, *Talanta*, 2024, **266**, 124979.

[13] P. Huo, Z. Li, R. Yao, Y. Deng, C. Gong, D. Zhang, C. Fan and S. Pu, Dual-ligand lanthanide metal–organic framework for ratiometric fluorescence detection of the anthrax biomarker dipicolinic acid, S*pectrochim Acta A,* 2022, **282**, 121700.

[14] Y. Xu, X. Shi, F. Ran, Z. Zhang, J. Phipps, X. Liu and H. Zhang, Differential sensitization toward lanthanide metal–organic framework for detection of an anthrax biomarker, *Microchim. Acta*, 2022, **190**, 27.